

1 **SUPPLEMENTARY MATERIAL**

2 Selection, biophysical and structural analysis of synthetic nanobodies that  
3 effectively neutralize SARS-CoV-2

4 Tânia F. Custódio<sup>1</sup>, Hrishikesh Das<sup>2</sup>, Daniel J Sheward<sup>3,4</sup>, Leo Hanke<sup>3</sup>, Samuel Pazicky<sup>1</sup>,  
5 Joanna Pieprzyk<sup>1</sup>, Michèle Sorgenfrei<sup>5</sup>, Martin A. Schroer<sup>6</sup>, Andrey Yu. Gruzinov<sup>6</sup>, Cy M.  
6 Jeffries<sup>6</sup>, Melissa A. Graewert<sup>6</sup>, Dmitri I. Svergun<sup>6</sup>, Nikolay Dobrev<sup>7</sup>, Kim Remans<sup>7</sup>, Markus  
7 A. Seeger<sup>5</sup>, Gerald M McInerney<sup>3</sup>, Ben Murrell<sup>3\*</sup>, B. Martin Hällberg<sup>2,8\*</sup> and Christian Löw<sup>1\*</sup>

8

9 <sup>1</sup> Centre for Structural Systems Biology (CSSB), DESY and European Molecular Biology  
10 Laboratory Hamburg, Notkestrasse 85, D-22607 Hamburg, Germany.

11 <sup>2</sup> Centre for Structural Systems Biology (CSSB) and Karolinska Institutet VR-RÅC,  
12 Notkestrasse 85, D-22607 Hamburg, Germany.

13 <sup>3</sup> Department of Microbiology, Tumor and Cell Biology, Karolinska Institutet, Stockholm  
14 17177, Sweden.

15 <sup>4</sup> Division of Virology, Institute of Infectious Diseases and Molecular Medicine, Faculty of  
16 Health Sciences, University of Cape Town, South Africa.

17 <sup>5</sup> Institute of Medical Microbiology, University of Zurich, Switzerland.

18 <sup>6</sup> European Molecular Biology Laboratory (EMBL), Hamburg Outstation c/o Deutsches  
19 Elektronen Synchrotron (DESY), Notkestrasse 85, D-22607 Hamburg, Germany.

20 <sup>7</sup> European Molecular Biology Laboratory (EMBL) Heidelberg, Protein Expression and  
21 Purification Core Facility, 69117 Heidelberg, Germany.

22 <sup>8</sup> Department of Cell and Molecular Biology, Karolinska Institutet, 17177 Stockholm, Sweden.

23

24

25

26

27

28

29

30

31

32

33 **Supplementary Table 1 – Summary of affinity measurements and neutralization assays**

34

	$K_D$ (nM)	$IC_{50}$ ( $\mu$ g/ml)
Sb12	$24.2 \pm 4.5$	3.7
Sb23	$10.6 \pm 2.0$	0.6
Sb23-Fc	$0.22 \pm 0.0001$	0.007
Sb42	$5.0 \pm 0.9$	1.1
Sb42-Fc	$0.19 \pm 0.00002$	0.07
Sb76	$58.1 \pm 11.4$	9.05
Sb95	$43.9 \pm 11.9$	ND
Sb100	$38.7 \pm 5.6$	2.4
Sb23/12	$0.53 \pm 0.0004$	0.008

35

36

37

38

39

40

41

42

43

44

45

46

47

48

49

50

51

52

53

54

55

56 **Supplementary Table 2 – Sequence of primers used in this study**

57

Primers for PCR amplification of pCMVExt-Fc plasmid	Fw gacaaaactcacacatgcc Rv ggatccctgaaaatacaggttt
SLIC cloning Sb23-Fc or Sb42-Fc: Primers to amplify Sb23 or Sb42	Fw gaaaacctgtatttcagggatcccagggtcagctggtgag Rv cggtgggcatgtgtgagttttgctcctcacagtcacttgggt
SLIC cloning Sb23/Sb12: Primers to amplify Sb12 and introduce a GS linker	Fw_1 ggcggtagcggcggaggaggcagcggaggacaggtcagctggtgag Rv_1 gctcacagtcacttgggtac Fw_2 caaggtacccaagtactgtgagcggaggaggcggtagcggcgga Rv_2 cctctctgagatgagttttgctcagctcttctcgcctcacagtcacttgggt
Mutagenic primers to introduce a HindIII restriction site on pSBinit plasmid containing Sb23	Fw tgactgtgagcgcaggaaaagcttgcaacaaaaactcat Rv atgagttttgttcgcaagcttttctcgcctcacagtc

58

59

60

61

62

63

64

65

66

67

68

69

70

71

72

73

74

75

76

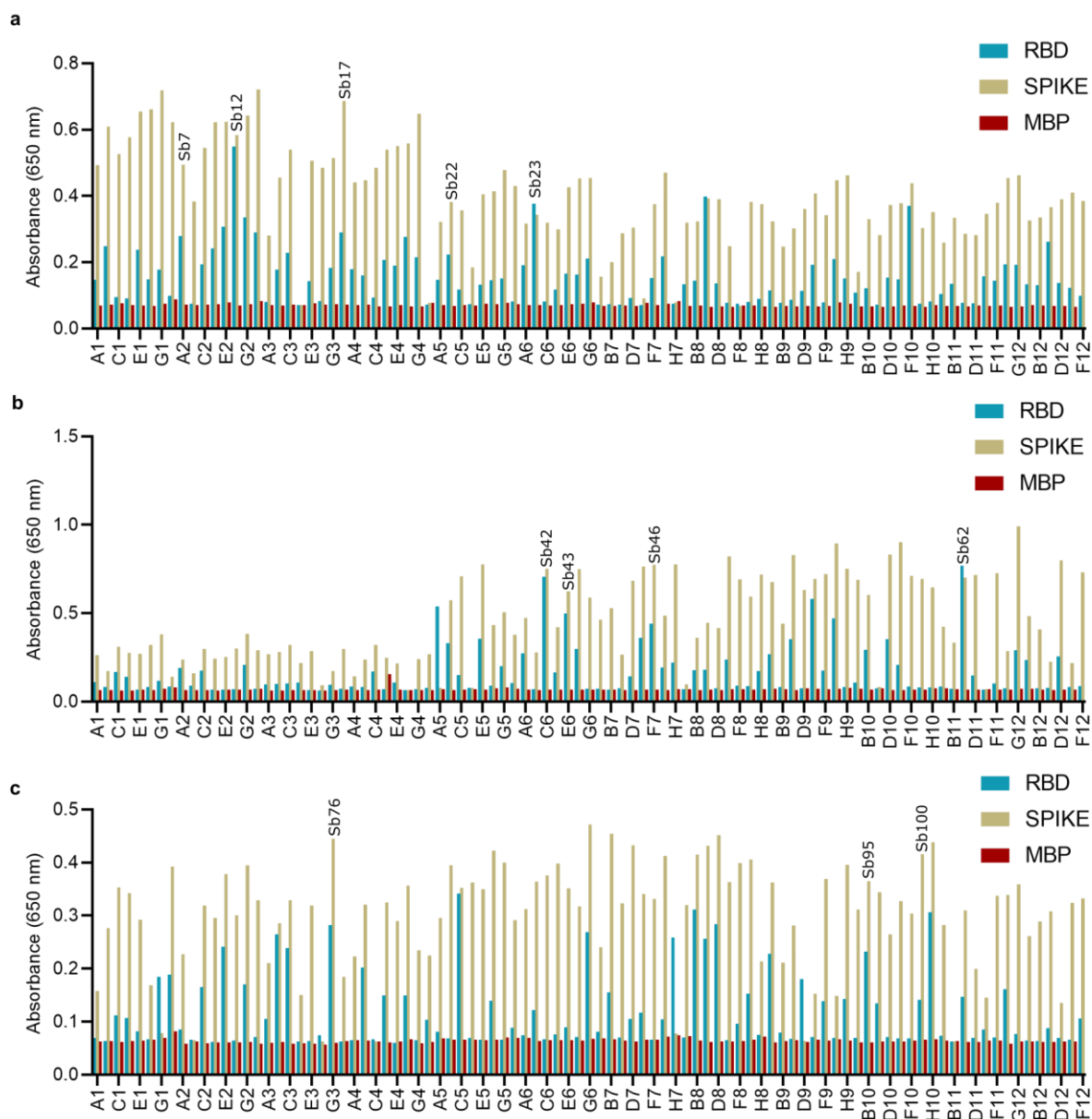
77

78

79

80

81 **Supplementary Fig. 1**



82

83

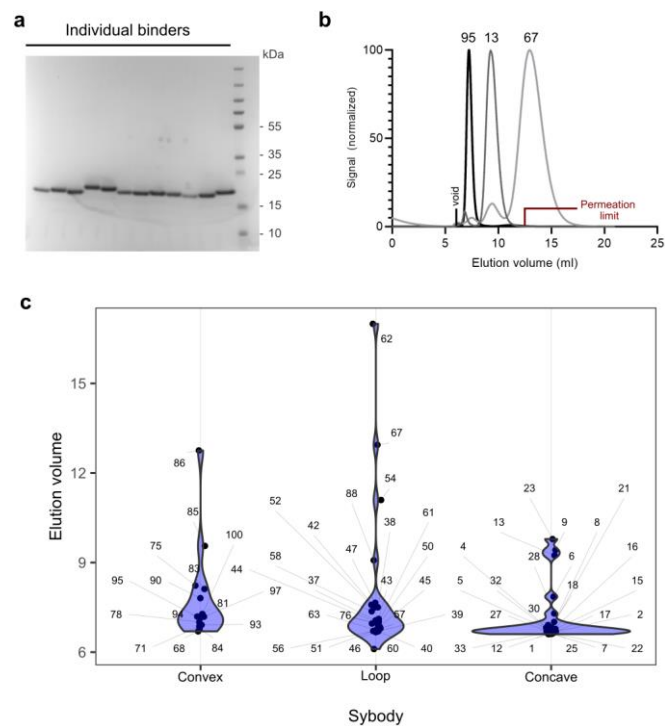
84 **RBD-specific sybodies were determined by ELISA.**

85 94 individual colonies from each of the three libraries, concave **(a)**, loop **(b)** and convex **(c)**  
 86 were randomly selected and screened against the two target proteins, RBD and spike. The same  
 87 procedure was performed for the MBP, used as background control signal. RBD or spike  
 88 signals with ratios above 1.5 compared to the MBP signal, were considered as hits. The  
 89 corresponding ELISA signals are labelled according to the sybodies that were illustrated or  
 90 characterized in this work.

91

92

93 **Supplementary Fig. 2**



94

95

96 **Expression and Purification of 62 unique sybodies.**

97 From 85 unique binders, 62 were expressed and purified. The purified sybodies were analysed  
98 by SDS-PAGE (**a**) and gel filtration using a SRT SEC-100 column (**b**). Sybodies 12, 23, 42,  
99 76, 95, and 100 were expressed and analysed at least two independent times. All other sybodies  
100 were only expressed and analysed once. Very few sybodies exhibit column interaction (sticky  
101 binders), eluting at or after the permeation limit of columns. **c** Elution volume of all purified  
102 binders, grouped by library.

103

104

105

106

107

108

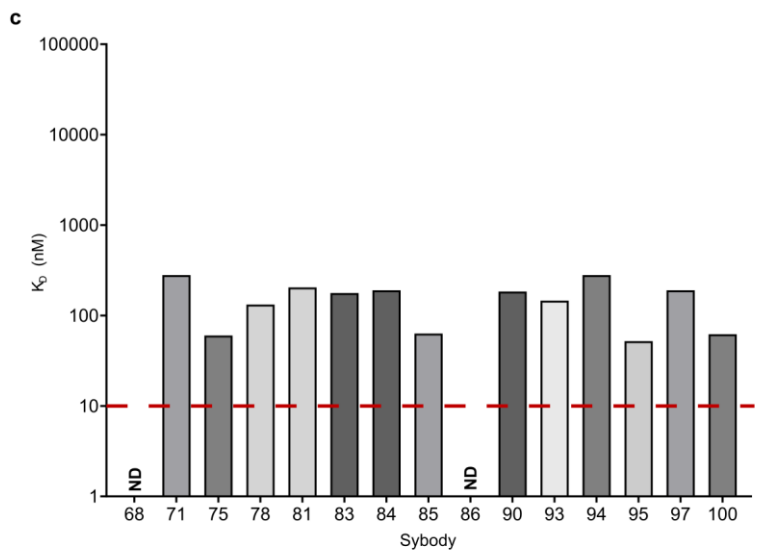
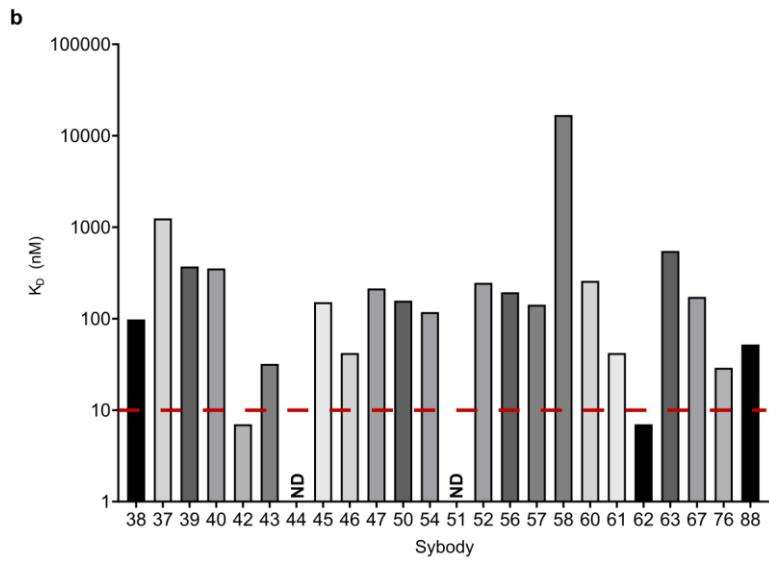
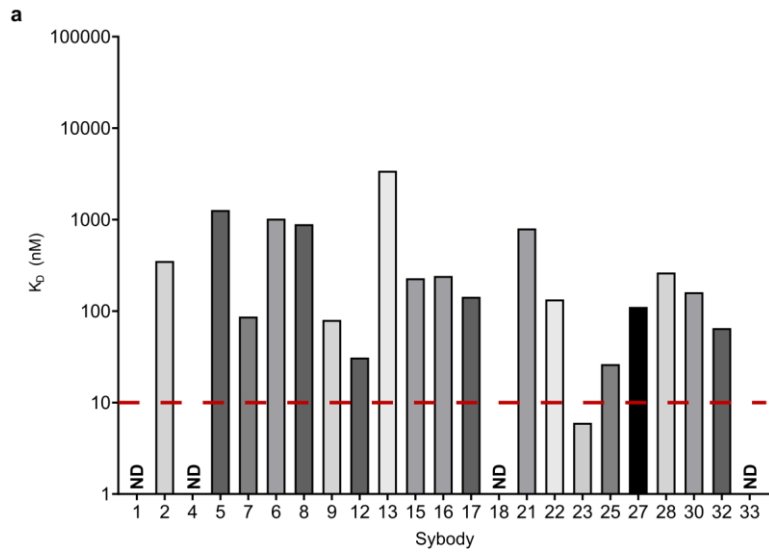
109

110

111

112

113



117 **Affinity screening of 62 sybodies.**

118 BLI sensorgrams of immobilized SARS-CoV-2 RBD with individual sybodies were recorded  
119 at one concentration (500 nM). The binding curves were fitted to a 1:1 binding model and  $K_D$   
120 values were estimated and plotted according to the different libraries concave (**a**), loop (**b**) and  
121 convex (**c**). ND, not determined. The most promising binders, further characterized in this  
122 study, are highlighted.

123

124

125

126

127

128

129

130

131

132

133

134

135

136

137

138

139

140

141

142

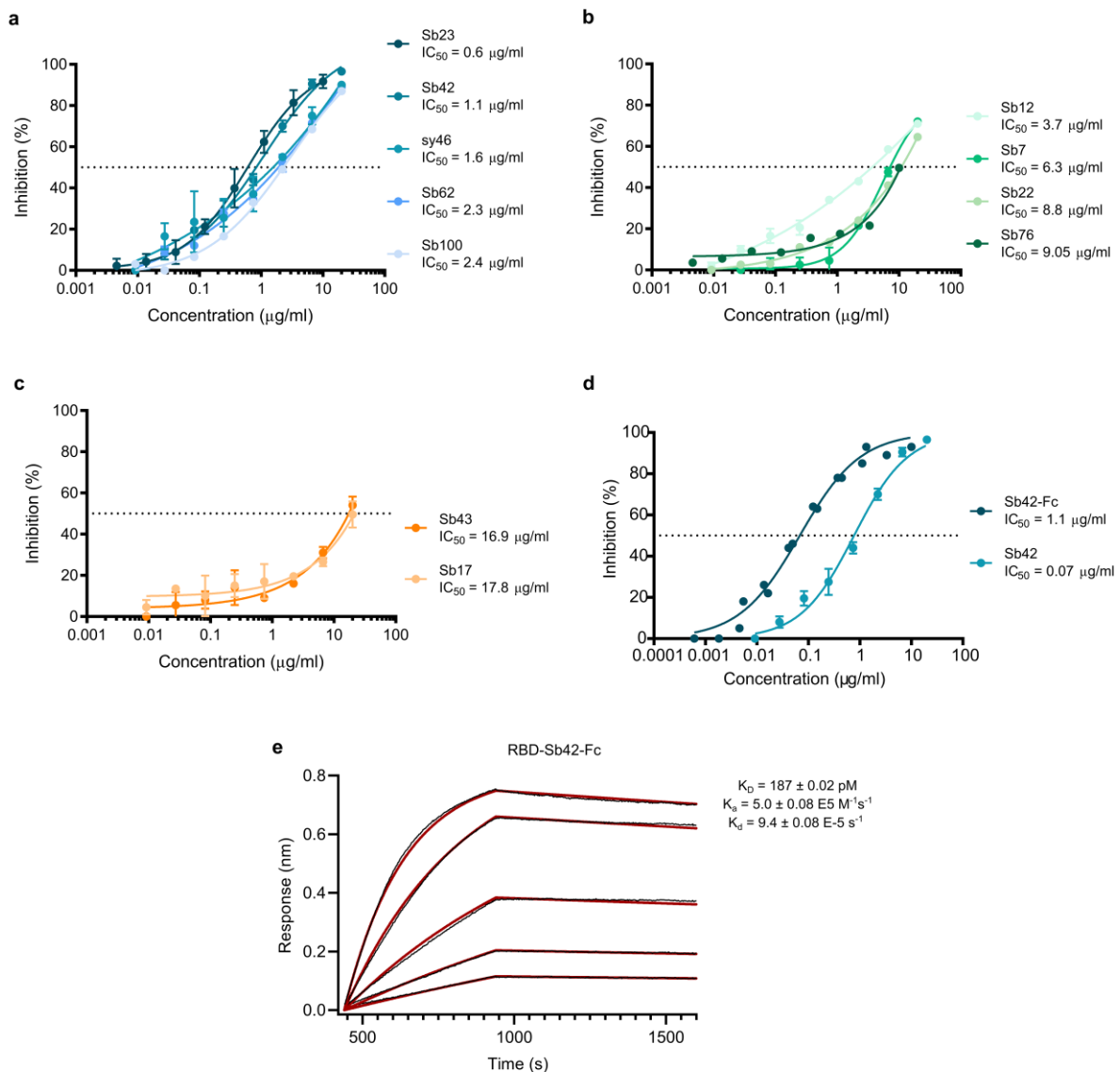
143

144

145

146

147



149

150 **Neutralization capacity of selected sybodies.**

151 SARS-CoV-2 pseudoviruses were incubated with a dilution series of target sybody and  
 152 grouped according to sybodies that showed the lowest IC<sub>50</sub> values (**a**), sybodies that showed  
 153 IC<sub>50</sub> values above 3 μg/ml (**b**) or sybodies that showed IC<sub>50</sub> values above 10 μg/ml (**c**). **d**  
 154 Neutralization potential of Sb42 is increased when fused to an antibody-derived Fc domain.  
 155 Data for all assays are mean ± SD of two replicate experiments. **e** BLI sensorgrams of  
 156 immobilized SARS-CoV-2 RBD with 2-fold serial dilution of 20 nM Sb42-Fc.

157

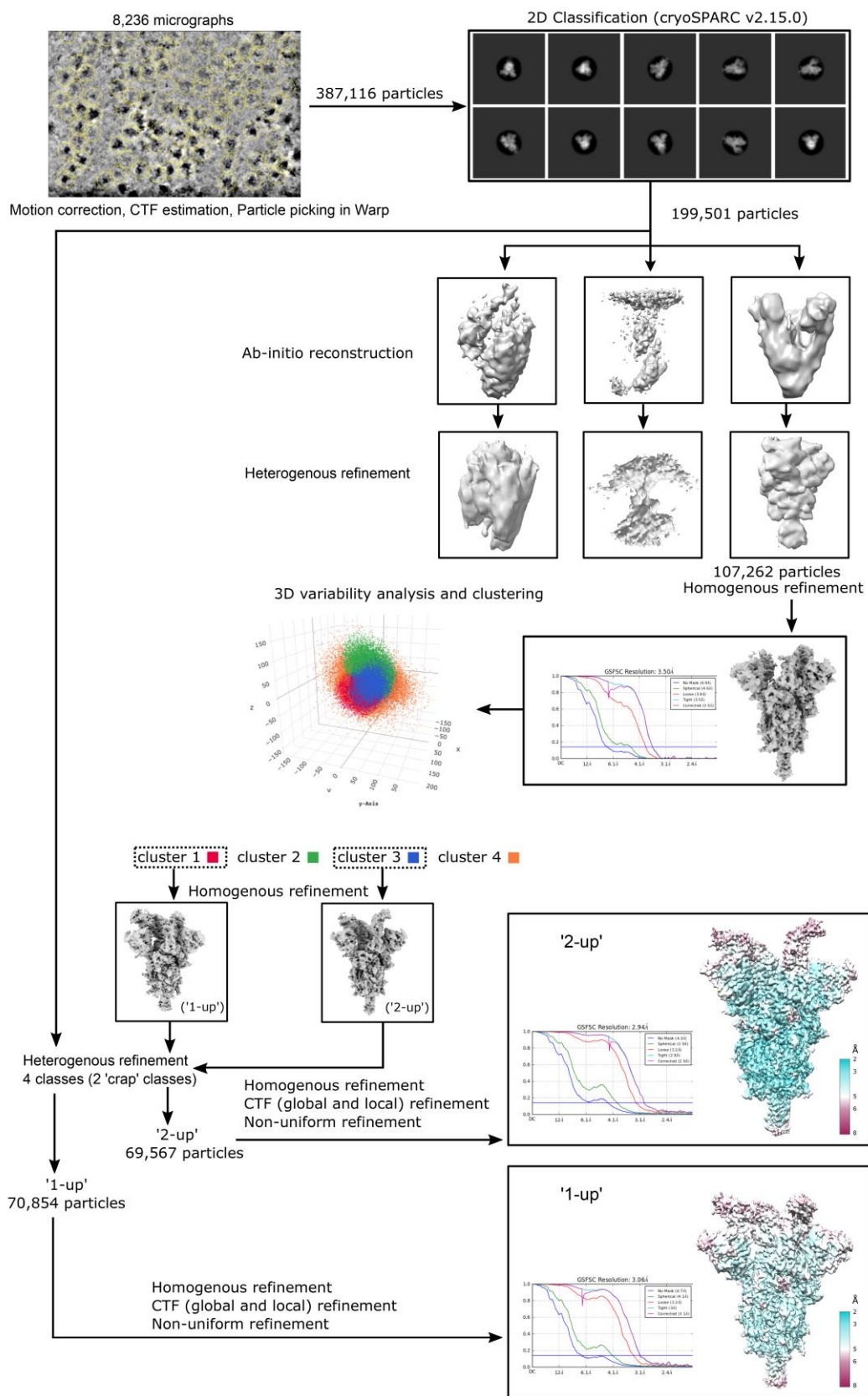
158

159

160



161 **Supplementary Fig. 5**



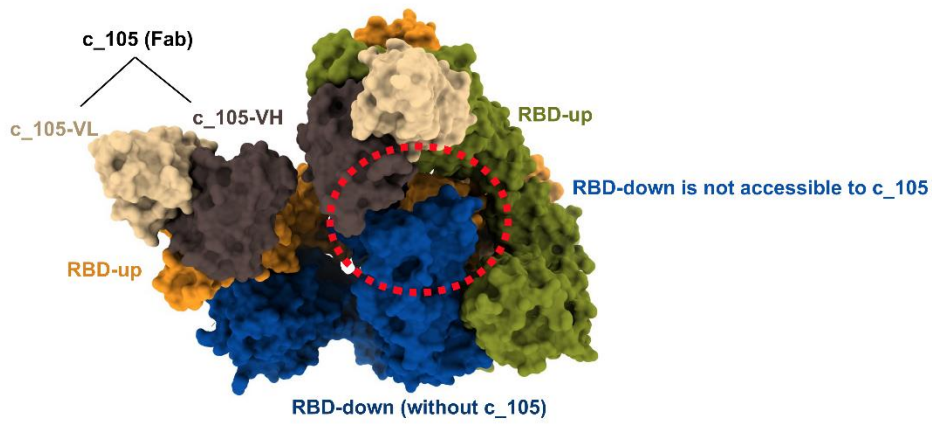
162

163 **Overview: EM processing performed for the '1-up' and '2-up' reconstructions.**

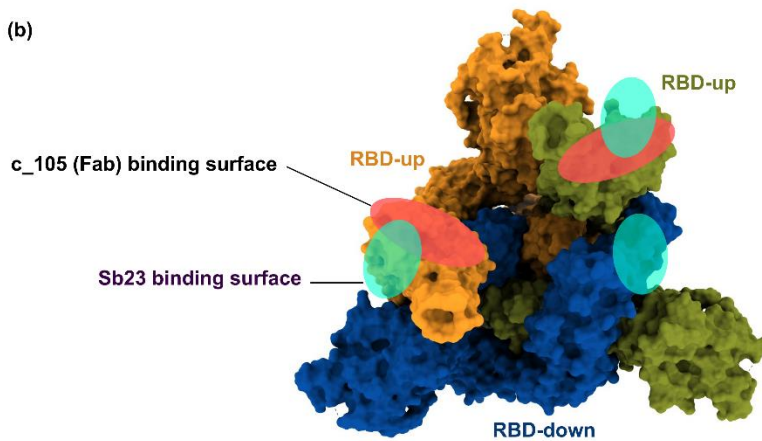
164 For clarity, the representative micrograph is denoised using Warp<sup>1</sup>.

165 **Supplementary Fig. 6**

(a)



(b)



166

167 **Comparison of Sb23 and FAB\_C105 binding.**

168 (a) Cryo-EM reconstruction of FAB\_C105<sup>2</sup> that shows that binding of the RBD in the down  
169 state is sterically occluded. (b) top view of SARS-CoV-2 spike showing and comparing the  
170 epitopes of Sb23 and FAB\_C105.

171

172

173

174

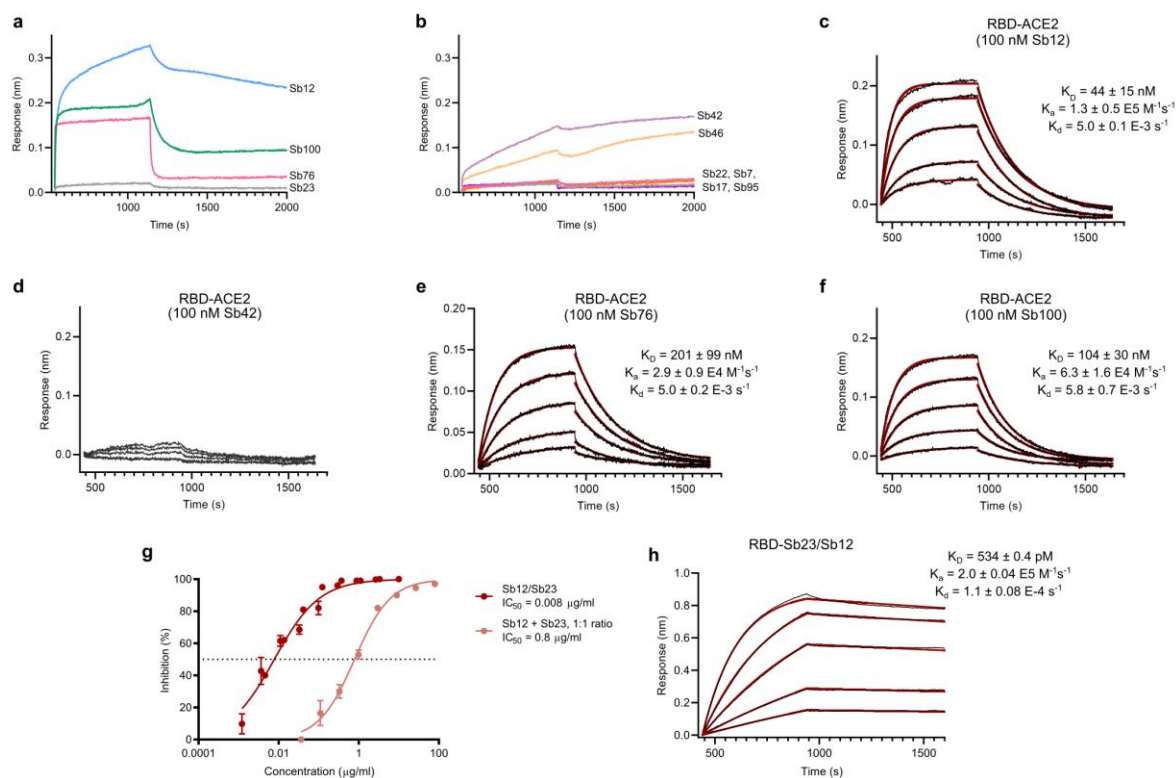
175

176

177

178

179 **Supplementary Fig. 7**



180

181 **Selected sybodies recognize two distinct epitopes on RBD**

182 BLI sensorgrams of immobilized SARS-CoV-2 RBD in the presence of 100 nM Sb23 with 750  
 183 nM of the indicated sybody. Sb12, 76 and 100 recognize a different epitope on RBD than Sb23  
 184 **(a)** while the other screened sybodies appear to have the same or overlapping epitopes **(b)**. BLI  
 185 sensorgrams of immobilized SARS-CoV-2 RBD with ACE2 in the presence 100 nM Sb12 **(c)**,  
 186 or 100 nM Sb42 **(d)**, or 100 nM Sb76 **(e)**, or 100 nM Sb100 **(f)**. The assay was performed in a  
 187 concentration range of 200-12.5 nM ACE2 and fit of the data to a 1:1 binding model is shown  
 188 in red. **g** SARS-CoV-2 spike pseudotyped lentivirus was incubated with a dilution series of  
 189 Sb23/Sb12 or Sb23 plus Sb12 added in 1:1 molar ratio. The assay was repeated at least in  
 190 duplicates and the error bars represent the standard deviation. **h** BLI sensorgrams of  
 191 immobilized SARS-CoV-2 RBD with 2-fold serial dilution of 30 nM Sb23/Sb12.

192

193

194

195

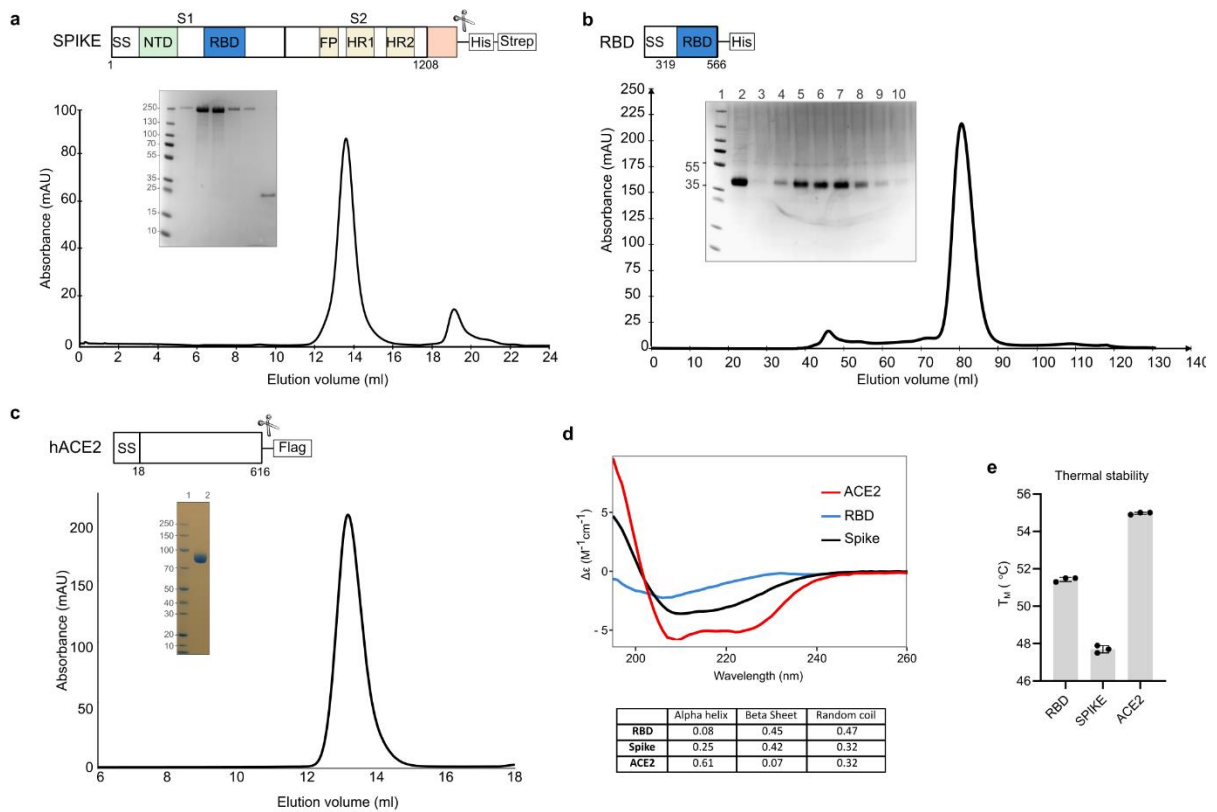
196

197

198

199 **Supplementary Fig. 8**

200



201

202

203 **Purification and biophysical characterization of antigens.**

204 Purified proteins showed no signs of aggregation and remained stable and monodisperse. **a**  
 205 Schematic illustration of the SARS-CoV-2 spike protein. Subunit S1 comprises the N-terminal  
 206 signal sequence (SS), the N-terminal domain (NTD) and the Receptor Binding Domain (RBD),  
 207 while subunit S2 consists of the fusion peptide (FP) and two heptad repeats, HR1 and HR2. At  
 208 the C-terminus the construct contains a T4 fibrin trimerization motif, followed by a HRV3C  
 209 protease cleavage site, an 8×Histidine tag and a Twin-Strep tag. Representative gel-filtration  
 210 chromatogram of the spike protein. Inset: Instant blue-stained SDS-PAGE analysis of the size  
 211 exclusion chromatography run. Lane 1: protein molecular weight marker. Lanes 2 - 6: fractions  
 212 eluted from the Superose 6 column. Line 7: fractions contained 3C protease. **b** The RBD  
 213 comprising residues 319 - 566 was used for sybody selections. A representative gel-filtration  
 214 chromatogram of RBD is shown. Inset: Instant blue-stained SDS-PAGE analysis of the size  
 215 exclusion chromatography run. Lane 1: protein molecular weight marker. Line 2: pooled  
 216 fractions from IMAC purification. Lanes 3 - 10: fractions eluted from the HiLoad Superdex  
 217 200 column. **c** The human receptor ACE2 comprising residues 18 - 616 was used for  
 218 competition assays. A representative gel-filtration chromatogram of the ACE2 protein is

219 shown. Inset: Instant blue-stained SDS-PAGE analysis of the size exclusion chromatography  
220 run. Lane 1: protein molecular weight marker. Lane 2 pooled fractions eluted from the  
221 Superdex 200 column. All the three proteins (RBS, Spike and ACE2) were expressed and  
222 purified at least three times and showed identical SEC profiles. **d** Far-UV-CD spectra of the  
223 human ACE2 receptor (red), SARS-CoV-2 RBD (blue) and SARS-CoV-2 spike (black) with  
224 the corresponding secondary structure content. **e** Thermal stability analysis of RBD, spike and  
225 ACE2. Data represents the mean  $\pm$  SD of three replicate experiments.

226  
227  
228  
229  
230  
231  
232  
233  
234  
235  
236  
237  
238  
239  
240  
241  
242  
243  
244  
245  
246  
247  
248  
249  
250  
251  
252

253 **References**

- 254 1. Tegunov, D. & Cramer, P. Real-time cryo – EM data pre-processing with Warp. *Nat.*  
255 *Methods* **16**, 1146–1152 (2020).
- 256 2. Barnes, C. O. *et al.* Structures of Human Antibodies Bound to SARS-CoV-2 Spike  
257 Reveal Common Epitopes and Recurrent Features of Antibodies. *Cell* **182**, 1–15  
258 (2020).
- 259